Inorganic Chemistry

Article

pubs.acs.org/IC

Heterometallic 3d−4f Coordination Polymers Based on 1,4,7-Triazacyclononane-1,4,7-triyl-tris(methylenephosphonate)

Yan-Hui Su, Song−Song Bao, and Li-Min Zheng*

State Key Laboratory of Coordination Chemistry, School of Chemistry and Chemical Engineering, Nanjing University, Nanjing 210093, China

Supporting Information

ABSTRACT: Five heterometallic 3d−4f coordination polymers based on 1,4,7-triazacyclononane-1,4,7-triyl-tris(methylenephosphonic acid) ($notpH_6$) are reported. Compounds $[FeLn(notpH)(H_2O)_4]ClO_4·5H_2O$ [Ln = Nd (**FeNd**), Gd (**FeGd**), Sm (**FeSm**), Eu (**FeEu**)] are isostructural. All show layer structures in which the $Fe(notpH)^{2-}$ unit serves as a metalloligand to link four equivalent Ln^{III} ions into a layer. Compound $[CuLa(notpH_2)(H_2O)_2]ClO_4·3H_2O$ (**CuLa**) displays a chain structure, where the $Cu(notpH_2)^{2-}$ unit connects the La^{III} ions into a chain. The magnetic properties of **FeLn** are studied.

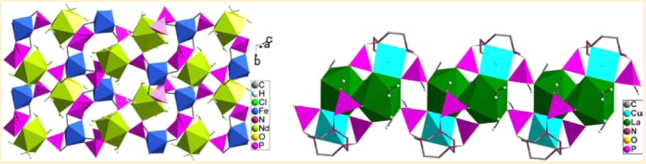

INTRODUCTION

The 3d−4f heterometallic coordination compounds have received increasing attention in recent years owing to their fascinating optical[1] and magnetic[2] properties. The incorporation of phosphonate ligands could not only enhance the thermal stabilities of the molecular systems but also produce new materials with versatile structures.[3] However, although a number of 3d−4f compounds have been reported so far, those containing phosphonate ligands are extremely rare.[4−7] Among the various approaches to assemble 3d−4f coordination polymers, the most efficient one is to employ N,O-containing ligands that can bind both the transition metal and lanthanide ions simultaneously. Indeed, by using 2-pyridylphosphonate, we succeeded in synthesizing a series of CuLn, ZnLn, and CoLn compounds with three-dimensional (3D) open-framework structures.[5] Sevov and co-workers obtained CuLa and CuNd compounds based on *N*-(phosphonomethyl)iminodiacetic acid, which show 3D framework structures.[6] The 1,4,7-triazacyclononane-1,4,7-triyl-tris(methylenephosphonic acid) ($notpH_6$) can provide three nitrogen and nine oxygen atoms as coordination donors. It can react with the transition metal,[8] lanthanide,[9] or actinide[8] ions forming coordination polymers. Stable mononuclear complexes such as $Fe(notpH_3)$[10] and $Cu(notpH_4)$[11] have also been reported. These mononuclear species can further act as metalloligands to connect the lanthanide ions into 3d−4f polymeric structures. This strategy has led to the isolation of a layered 3d−4f compound $[Is-Co^{III}La^{III}(notp)(H_2O)_4]·nH_2O$.[7] In this Paper, we report the first examples of FeLn and CuLn compounds based on $notpH_6$, namely, $[FeLn(notpH)(H_2O)_4]ClO_4·5H_2O$ [Ln = Nd (**FeNd**), Gd (**FeGd**), Sm (**FeSm**), Eu (**FeEu**)] and $[CuLa(notpH_2)(H_2O)_2]ClO_4·3H_2O$ (**CuLa**). The **FeLn** compounds are isostructural, showing layered structures, while the **CuLa** compound displays a chain structure. The magnetic properties are also investigated.

EXPERIMENTAL SECTION

Materials and Measurements. 1,4,7-Triazacyclononane-1,4,7-triyl-tris(methylenephosphonic acid) [$notpH_6$, $C_9H_{18}N_3(PO_3H_2)_3$] was prepared by a modified literature method.[12] Compounds $Fe(notpH_3)$[10] and $Cu(notpH_4)$[11] were synthesized using solution-diffusion method. All the other starting materials were obtained commercially as reagent grade chemicals and used without further purification. The elemental analyses for C, H, and N were performed in a PE240C elemental analyzer. The infrared (IR) spectra were recorded on a VECTOR 22 spectrometer with KBr pellets. The powder X-ray diffraction (XRD) patterns were recorded on a Shimadzu XD-3A X-ray diffractometer. Magnetic susceptibility data were obtained on polycrystalline samples (16.59 mg for **FeNd**, 7.12 mg for **FeSm**, 7.54 mg for **FeEu**, 7.26 mg for **FeGd**) using a Quantum Design MPMS-XL7 SQUID magnetometer. Diamagnetic corrections were made for both the sample holder and the compound estimated from Pascal's constants.[13]

Synthesis of $[FeLn(notpH)(H_2O)_4]ClO_4·5H_2O$ (FeLn, Ln = Nd, Gd, Sm, Eu). These compounds were prepared by a similar experimental procedure except that appropriate lanthanide(III) perchlorate hydrates were used. A typical procedure for the preparation of **FeNd** is described. To an aqueous solution of $Fe(notpH_3)$ (28 mg, 0.05 mmol) was added $Nd(ClO_4)_3·6H_2O$ (27.5 mg, 0.05 mmol). The mixture was stirred for 30 min, and then 1 M $HClO_4$ was dropped in until a clear solution was obtained (pH = 1.4). The filtrate was allowed to stand at room temperature for a week. Yellow lamellar crystals of **FeNd** were obtained as a monophasic material, judged by powder X-ray diffraction pattern. Yield: 22 mg (50% based on Nd). Anal. Calcd for $C_9H_{37}ClFeN_3NdO_{22}P_3$: C, 12.46; H, 4.15; N, 4.84. Found: C, 12.31; H, 3.89; N, 4.44%. IR (KBr, cm^{-1}): 3421(b), 1637(m), 1470(w), 1384(w), 1316(w), 1161(s), 1105(s), 1054(s), 1017(m), 996(m), 948(m), 777(w), 751(w), 591(m), 458(w), 427(w).

For **FeGd**: 26 mg (60% based on Gd). Anal. Calcd for $C_9H_{37}ClFeN_3GdO_{22}P_3$: C, 12.26; H, 4.19; N, 4.76. Found: C, 12.55;

Received: February 13, 2014
Published: June 4, 2014

dx.doi.org/10.1021/ic500356b | *Inorg. Chem.* 2014, 53, 6042−6047

Table 1. Crystallographic Data for FeNd, FeSm, and CuLa

	FeNd	FeSm	CuLa
empirical formula	$C_9H_{37}ClFeN_3NdO_{22}P_3$	$C_9H_{37}ClFeN_3SmO_{22}P_3$	$C_9H_{30}ClCuLaN_3O_{18}P_3$
fw	867.86	873.97	799.17
crystal system, space group	monoclinic, $P2_1/n$	monoclinic, $P2_1/n$	triclinic, $P\bar{1}$
a (Å)	17.490(5)	17.490(4)	9.332(2)
b (Å)	8.866(3)	8.815(2)	9.781(2)
c (Å)	19.076(6)	19.067(4)	14.514(4)
α (deg)			78.379(4)
β (deg)	110.661(4)	110.601(4)	80.923(4)
γ (deg)			70.905(4)
V (Å^3), Z	2767.9(14), 4	2751.7(10), 4	1220.1(5), 2
D_c (g cm^{-3})	2.083	2.110	2.175
μ (mm^{-1})	2.745	3.009	2.992
F (000)	1744	1752	794
$R1^a$,$wR2^b$ [$I > 2\sigma(I)$]	0.0441, 0.0896	0.0444, 0.0917	0.0362, 0.0766
$R1^a$,$wR2^b$ (all data)	0.0742, 0.1017	0.0634, 0.0944	0.0451, 0.0780
goodness-of-fit	1.003	0.975	0.992
$(\Delta\rho)$max, $(\Delta\rho)$min (e Å^{-3})	0.94, −0.91	1.12, −0.70	1.03, −0.78
CCDC number	982 015	982 014	982 016

$^aR_1 = \Sigma||F_o| - |F_c||/\Sigma|F_o|$. $^bwR_2 = [\Sigma w(F_o^2 - F_c^2)^2/\Sigma w(F_o^2)^2]^{1/2}$.

H, 3.76; N, 4.59%. IR (KBr, cm^{-1}): 3419(b), 1639(s), 1471(w), 1384(m), 1317(w), 1305(w), 1290(w), 1257(w), 1162(s), 1143(s), 1122(vs), 1108(s), 1081(s), 1058(s), 1020(m), 997(s), 952(m), 779(m), 752(m), 592(s), 424(w).

For **FeSm**: 24 mg (55% based on Sm). Anal. Calcd for $C_9H_{37}ClFeN_3SmO_{22}P_3$: C, 12.36; H, 4.23; N, 4.80. Found: C, 12.30; H, 3.98; N, 4.53%. IR (KBr, cm^{-1}): 3404(b), 1639(s), 1492(w), 1471(m), 1429(w), 1315(m), 1290(m), 1257(w), 1161(vs), 1105(vs), 1080(vs), 1058(vs), 1017(s), 997(s), 950(s), 779(s), 752(m), 592(s), 457(w), 426(w).

For **FeEu**: 20 mg (49% based on Eu). Anal. Calcd for $C_9H_{37}ClFeN_3SmO_{22}P_3$: C, 12.34; H, 4.22; N, 4.70. Found: C, 12.51; H, 3.61; N, 4.24%. IR (KBr, cm^{-1}): 3409(b), 1637(s), 1490(w), 1471(m), 1427(w), 1315(w), 1292(w), 1163(vs), 1130(vs), 1105(vs), 1180(vs), 1062(vs), 1018(s), 997(s), 948(s), 779(m), 752(w), 624(m), 592(s), 459(w), 426(w).

Thermal analyses reveal that the weight losses below 155 °C are 18.2% for **FeNd**, 18.2% for **FeGd**, 18.2% for **FeSm**, and 18.4% for **FeEu**, close to the removal of five lattice water molecules and four coordinated water molecules (calcd 18.7% for **FeNd**, 18.4% for **FeGd**, 18.5% for **FeSm**, 18.5% for **FeEu**).

Synthesis of $[CuLa(notpH_2)(H_2O)_2]ClO_4{\cdot}3H_2O$ (CuLa). To an aqueous solution of $Cu(notpH_4)$ (24 mg, 0.05 mmol) was added $La(ClO_4)_3{\cdot}6H_2O$ (21 mg, 0.05 mmol). The mixture was stirred for 1 h, and 1 M $HClO_4$ was dropped in until a clear solution was obtained. The filtrate was allowed to stand at room temperature for a week. Blue block crystals of **CuLa** were obtained as a monophasic material, judged by powder X-ray diffraction pattern. Yield: 26 mg (65% based on La). Anal. Calcd for $C_9H_{30}ClCuLaN_3O_{18}P_3$: C, 13.51; H, 3.75; N, 5.25. Found: C, 13.65; H, 3.68; N, 5.10%. IR (KBr, cm^{-1}): 3423(b), 2872(w), 2368(b), 1635(m), 1508(w), 1460(w), 1420(w), 1384(m), 1236(m), 1190(s), 1134(vs), 1116(vs), 1079(vs), 1006(s), 954(m), 786(m), 626(m), 577(s), 458(m). Thermal analysis reveals that the first step weight loss of **CuLa** in the temperature range 25−75 °C is 6.8%, in agreement with the removal of three lattice water molecules (calcd 6.8%). The second step weight loss (4.4%) occurs in the temperature range of 130−180 °C, corresponding to the release of two coordinated water molecules (calcd 4.5%).

X-ray Crystallographic Analyses. Single crystals with dimensions 0.20 × 0.12 × 0.06 mm^3 for **FeNd**, 0.16 × 0.10 × 0.06 mm^3 for **FeSm**, and 0.15 × 0.13 × 0.10 mm^3 for **CuLa** were selected for indexing and intensity data collection on a Bruker SMART APEX CCD diffractometer using graphite monochromatized Mo Kα radiation (λ = 0.710 73 Å) at room temperature. A hemisphere of data was collected in the θ range of 1.96−25.00° for **FeNd**, 1.96−25.00° for **FeSm**, and 2.23−25.05° for **CuLa** using a narrow-frame method with scan widths of 0.30° in ω and exposure time of 10 s/frame. Numbers of observed and unique reflections are 13 495 and 4862 (R_{int} = 0.0715) for **FeNd**, 13 213 and 4830 (R_{int} = 0.0883) for **FeSm**, and 6139 and 4237 (R_{int} = 0.0424) for **CuLa**, respectively. The data were integrated using the Siemens SAINT program,[14] with the intensities corrected for Lorentz factor, polarization, air absorption, and absorption due to variation in the path length through the detector faceplate. Absorption corrections were applied. The structures were solved by direct methods and refined on F^2 by full matrix least-squares using SHELXTL.[15] All non-hydrogen atoms were located from the Fourier maps and refined anisotropically. All the hydrogen atoms were put on calculated positions or located from the Fourier maps and refined isotropically with the isotropic vibration parameters related to the non-H atom to which they are bonded. Crystallographic data are listed in Table 1. The selected bond lengths and angles for compounds **FeNd**, **FeSm**, and **CuLa** are given in Tables 2−4, respectively.

RESULTS AND DISCUSSION

Crystal Structures of FeLn (Ln = Nd, Gd, Sm, Eu). Compounds **FeLn** (Ln = Nd, Gd, Sm, Eu) are isostructural according to their XRD patterns (Supporting Information, Figure S6). Single-crystal structural determinations were conducted for compounds **FeNd** and **FeSm**. Compound **FeNd** crystallizes in monoclinic space group $P2_1/n$. As shown in Figure 1a, the asymmetric building unit consists of one Fe^{III}, one Nd^{III}, one $notpH^{5-}$, one ClO_4^-, four coordinated and five lattice water molecules. The Fe1 atom is six-coordinated by three nitrogen (N1, N2, N3) and three phosphonate oxygen (O1, O4, O7) atoms from the same $notpH^{5-}$ ligand and displays a distorted octahedral geometry. The Fe−O bond distances fall in the range of 1.930(4)−1.960(4) Å, while the Fe−N bond distances are between 2.176(6) and 2.187(6) Å. The Nd1 atom is eight-coordinated, surrounded by four phosphonate oxygen atoms (O6, O3A, O2C, O9B) from four equivalent $notpH^{5-}$ ligands and four water oxygen (O1W, O2W, O3W, and O4W), forming a bicapped triprismatic geometry. The Nd−O bond distances are in the range of 2.350(5)−2.626(5) Å.

Each $notpH^{5-}$ acts as a decadentate ligand. It chelates the Fe atom using its three nitrogen and three phosphonate oxygen

dx.doi.org/10.1021/ic500356b | Inorg. Chem. 2014, 53, 6042−6047

Table 2. Selected Bond Lengths (Å) and Angles (deg) for FeNd[a]

Fe1−O1	1.930(4)	Fe1−O7	1.948(4)
Fe1−O4	1.960(4)	Fe1−N3	2.176(6)
Fe1−N1	2.187(5)	Fe1−N2	2.185(5)
Nd1−O3A	2.350(5)	Nd1−O9B	2.360(4)
Nd1−O6	2.373(5)	Nd1−O2C	2.395(4)
Nd1−O3W	2.535(5)	Nd1−O4W	2.546(6)
Nd1−O2W	2.556(4)	Nd1−O1W	2.626(5)
O1−Fe1−O7	97.7(2)	O1−Fe1−O4	96.3(2)
O7−Fe1−O4	100.8(2)	O1−Fe1−N3	165.5(2)
O7−Fe1−N3	84.3(2)	O4−Fe1−N3	97.4(2)
O1−Fe1−N1	84.7(2)	O7−Fe1−N1	95.3(2)
O4−Fe1−N1	163.6(2)	N3−Fe1−N1	80.8(2)
O1−Fe1−N2	95.8(2)	O7−Fe1−N2	165.2(2)
O4−Fe1−N2	83.7(2)	N3−Fe1−N2	81.1(2)
N1−Fe1−N2	79.9(2)	O3A−Nd1-O9B	87.4(2)
O3A−Nd1−O6	151.6(1)	O9B−Nd1−O6	98.8(2)
O3A−Nd1−O2B	92.6(2)	O9B−Nd1−O2C	150.5(1)
O6−Nd1−O2C	95.2(1)	O3A−Nd1−O3W	139.9(2)
O9B−Nd1−O3W	81.1(2)	O6−Nd1−O3W	68.5(2)
O2C−Nd1−O3W	80.0(1)	O3A−Nd1−O4W	72.6(2)
O9B−Nd1−O4W	80.0(2)	O6−Nd1−O4W	135.7(2)
O2C−Nd1−O4W	71.9(2)	O3W−Nd1−O4W	67.6(2)
O3A−Nd1−O2W	76.6(2)	O9B−Nd1−O2W	138.5(2)
O6−Nd1−O2W	80.6(2)	O2C−Nd1−O2W	69.5(2)
O3W−Nd1−O2W	134.0(2)	O4W−Nd1−O2W	128.6(2)
O3A−Nd1−O1W	80.2(2)	O9B−Nd1−O1W	70.2(1)
O6−Nd1−O1W	76.0 (2)	O2C−Nd1−O1W	138.9 (1)
O3W−Nd1−O1W	129.7(2)	O4W−Nd1−O1W	140.2(2)
O2W−Nd1−O1W	69.4(2)		

[a]Symmetry codes: A: $-x, -y, -z$; B: $-x + 1/2, y - 1/2, -z + 1/2$; C: $x, y - 1, z$; D: $x, y + 1, z$; E: $-x + 1/2, y + 1/2, -z + 1/2$.

Table 3. Selected Bond Lengths (Å) and Angles (deg) for FeSm[a]

Fe1−O7	1.931(4)	Fe1−O5	1.950(4)
Fe1−O1	1.953(4)	Fe1−N2	2.176(6)
Fe1−N1	2.193(6)	Fe1−N3	2.198(5)
Sm1−O4A	2.323(4)	Sm1−O8B	2.327(4)
Sm1−O9C	2.339(5)	Sm1−O3	2.350(5)
Sm1−O2W	2.515(5)	Sm1−O1W	2.517(5)
Sm1−O3W	2.548(4)	Sm1−O4W	2.586(5)
O7−Fe1−O5	97.0(2)	O7−Fe1−O1	96.3(2)
O5−Fe1−O1	100.2(2)	O7−Fe1−N2	165.4(2)
O5−Fe1−N2	84.7(2)	O1−Fe1−N2	97.6(2)
O7−Fe1−N1	97.4(2)	O5−Fe1−N1	164.7(2)
O1−Fe1−N1	83.5(2)	N2−Fe1−N1	80.0(2)
O7−Fe1−N3	85.1(2)	O5−Fe1−N3	96.3(2)
O1−Fe1−N3	163.2(2)	N2−Fe1−N3	80.3(2)
N1−Fe1−N3	79.7(2)	O4A−Sm1−O8B	88.6(2)
O4A−Sm1−O9C	150.8(2)	O8B−Sm1−O9C	94.8 (2)
O4A−Sm1−O3	97.2(2)	O8B−Sm1−O3	151.1 (2)
O9C−Sm1−O3	93.4(2)	O4A−Sm1−O2W	81.1(2)
O8B−Sm1−O2W	72.5(2)	O9C−Sm1−O2W	72.4(2)
O3−Sm1−O2W	136.3(2)	O4A−Sm1−O1W	80.3(2)
O8B−Sm1−O1W	139.5(2)	O9C−Sm1−O1W	78.3(2)
O3−Sm1−O1W	69.3(2)	O2W−Sm1−O1W	67.4(2)
O4A−Sm1−O3W	139.2(2)	O8B−Sm1−O3W	77.4(2)
O9C−Sm1−O3W	69.4 (2)	O3−Sm1−O3W	79.6(2)
O2W−Sm1−O3W	128.4(2)	O1W−Sm1−O3W	133.4(2)
O4A−Sm1−O4W	70.5(2)	O8B−Sm1−O4W	79.2(2)
O9C−Sm1−O4W	138.6(2)	O3−Sm1−O4W	76.4(2)
O2W−Sm1−O4W	140.1(2)	O1W−Sm1−O4W	131.1(2)
O3W−Sm1−O4W	69.3(2)		

[a]Symmetry codes: A: $-x + 1/2, y - 1/2, -z + 3/2$; B: $-x, -y, -z + 1$; C: $x, y - 1, z$; D: $-x + 1/2, y + 1/2, -z + 3/2$; E: $x, y + 1, z$.

atoms to give a mononuclear unit of $Fe(notpH)^{2-}$. Each $Fe(notpH)^{2-}$ behaves as a metalloligand and links four equivalent Nd atoms through its four phosphonate oxygen (O2, O3, O6, O9) atoms. The remaining two phosphonate oxygen atoms are either pendent (O8) or protonated (O5). Two equivalent $\{NdO_8\}$ polyhedra are each corner-shared with $\{PO_3C\}$ tetrahedra, forming a dimer of Nd_2P_2 with four-member ring. Each Nd_2P_2 dimer is connected to six $\{FeO_3N_3\}$ octahedra, while each $\{FeO_3N_3\}$ is linked to three Nd_2P_2 dimers via phosphonate groups. Therefore, a two-dimensional heterometallic layer structure is constructed that contains 4- and 16-member rings (Figure 1b). The Nd···Nd separation across O−P−O bridges is 5.478(1) Å, while the Fe···Nd distances are 5.513(2), 5.670(2), 5.831(2), and 6.432(2) Å, respectively. The positively charged layers are packed along the [101] direction. The perchlorate anions and lattice water molecules fill in the interlayer space (Figure 1c). Extensive hydrogen-bond interactions are found among the coordinated and lattice water molecules, the ClO_4^- anions as well as the phosphonate oxygen atoms within the layer and between the layers.

The structure of **FeSm** is analogous to that of **FeNd** described above except that the Nd atom is replaced by Sm atom. Owing to the lanthanide contraction effect, the cell volume of **FeSm** is slightly reduced. The Fe−O(N) distances [1.931(4)−2.198(5) Å] are in agreement with those in **FeNd**. The Sm−O bond distances are in the range of 2.323(4)−2.586(5) Å. Within the layer, the Sm···Sm separation across the O−P−O bridges is 5.375(1) Å, while the Fe···Sm distances are 5.551(1), 5.638(1), 5.792(1), and 6.399(1) Å, respectively.

Crystal Structure of CuLa. Compound **CuLa** crystallizes in the triclinic space group $P\bar{1}$. The asymmetric unit is composed of one Cu^{II}, one La^{III}, one $notpH_2^{4-}$, one ClO_4^-, two coordinated and three lattice water molecules (Figure 2a). The Cu1 atom has a distorted square pyramidal environment. The basal sites are occupied by two phosphonate oxygens (O3, O7) and two nitrogen atoms (N1, N3) from $notpH_2^{4-}$. The axial site is filled with the remaining nitrogen atom (N2) from the same $notpH_2^{4-}$ ligand. The axial Cu−N bond distance [2.299(5) Å] is longer than the basal Cu−N(O) distances [1.953(4)−2.016(5) Å] due to the Jahn−Teller effect. These bond distances are consistent with those in mononuclear compound $Cu(notpH_4)$.[11] The La1 atom is nine-coordinated, surrounded by seven phosphonate oxygen (O3, O6, O7, O1A, O5A, O6A, and O9B) from three $notpH_2^{4-}$ ligands and two water molecules (O1W, O2W), displaying a tricapped triprismatic geometry. The La−O bond distances fall in the range of 2.461(4)−2.803(4) Å, which are in agreement with those in the other phosphonate compounds.[16]

Each $notpH_2^{4-}$ acts as a nonadentate ligand with two phosphonate oxygen atoms (O4 and O8) protonated. It chelates the Cu atom through phosphonate oxygen atoms (O3, O7) and nitrogen atoms (N1, N2, and N3) to establish a mononuclear $Cu(notpH_2)^{2-}$ unit. Then the mononuclear unit further bridges the La atom by using its phosphonate oxygen atoms, forming an infinite chain structure (Figure 2b). Both O3

dx.doi.org/10.1021/ic500356b | Inorg. Chem. 2014, 53, 6042−6047

Table 4. Selected Bond Lengths (Å) and Angles (deg) for CuLa[a]

Cu1–O7	1.953(4)	Cu1–O3	1.989(4)
Cu1–N3	2.013(5)	Cu1–N1	2.016(5)
Cu1–N2	2.299(5)	La1–O6	2.450(4)
La1–O9A	2.461(4)	La1–O1B	2.481(4)
La1–O1W	2.550(4)	La1–O2W	2.590(4)
La1–O3	2.615(4)	La1–O5B	2.638(4)
La1–O7	2.666(3)	La1–O6B	2.803(4)
O7–Cu1–O3	87.5(2)	O7–Cu1–N3	89.9(2)
O3–Cu1–N3	161.5(2)	O7–Cu1–N1	167.8(2)
O3–Cu1–N1	91.5(2)	N3–Cu1–N1	87.2(2)
O7–Cu1–N2	107.5(2)	O3–Cu1–N2	115.6(2)
N3–Cu1–N2	82.6(2)	N1–Cu1–N2	83.9(2)
O6–La1–O9A	81.8(1)	O6–La1–O1B	78.5(1)
O9A–La1–O1B	74.0(1)	O6–La1–O1W	137.9(1)
O9A–La1–O1W	113.2(1)	O1B–La1–O1W	142.5(1)
O6–La1–O2W	151.8(1)	O9A–La1-O2W	79.0(1)
O1B–La1–O2W	76.4(1)	O1W–La1–O2W	69.5(1)
O6–La1–O3	67.8(1)	O9A–La1–O3	123.4(1)
O1B–La1–O3	137.5(1)	O1W–La1–O3	71.4(1)
O2W–La1–O3	140.4(1)	O6–La1–O5B	119.8(1)
O9A–La1–O5B	146.0(1)	O1B–La1–O5B	84.5(1)
O1W–La1–O5B	69.8(1)	O2W–La1–O5B	70.5(1)
O3–La1–O5B	90.2(1)	O6–La1–O7	83.7(1)
O9A–La1–O7	68.1(1)	O1B–La1–O7	140.0(1)
O1W–La1–O7	68.1(1)	O2W–La1–O7	107.7(1)
O3–La1–O7	62.2(1)	O5B–La1–O7	135.0(1)
O6–La1–O6B	66.6(1)	O9A–La1–O6B	137.9(1)
O1B–La1–O6B	73.0(1)	O1W–La1–O6B	108.9(1)
O2W–La1–O6B	117.1(1)	O3–La1–O6B	70.3(1)
O5B–La1–O6B	53.2(1)	O7–La1–O6B	130.7(1)

[a]Symmetry codes: A: $-x + 1, -y + 1, -z + 1$; B: $-x + 1, -y, -z + 1$.

and O7 serve as μ_3-O and link the Cu and La atoms into a dimer. The Cu···La distance within the dimer is 3.614(1) Å, and the Cu–O–La angles are 101.8(2) and 102.5(2)°. Besides, the equivalent La atoms are doubly bridged by μ_3-O6 [La–O–La angle: 113.3(2)°] and are further connected by the phosphonate groups to form an infinite chain (Figures 2b and 2c). The La···La distances are 4.394(1) Å over the μ_3-O6 bridge and 6.701(1) Å across the O–P–O units. Neighboring chains are connected by hydrogen bonds among the phosphonate oxygen and water molecules, leading to a layer in the *ab* plane (Supporting Information, Figure S10). These layers are packed along the *c*-axis, hence, constructing a three-dimensional supramolecular structure. Extensive hydrogen-bond interactions are present between the layers among the perchlorate anions, the lattice water molecules, and the phosphonate oxygen atoms (Figure 2d).

Obviously, the structure of **CuLa** is different from that of **FeLn**, although the synthetic procedures are quite similar in the two cases. Compound **CuLa** shows a chain structure, while a layer structure is found in **FeLn**. The structural difference could originate from both the charge and the coordination capabilities of the transition metal ions. The Cu^{II} has two positive charges and prefers a square-pyramidal coordination geometry, while the Fe^{III} has three positive charges and prefers an octahedral geometry. To balance the charge, two of the phosphonate oxygen atoms in the $notp^{6-}$ ligand are protonated in **CuLa**, while only one phosphonate oxygen atom is protonated in compound **FeLn**.

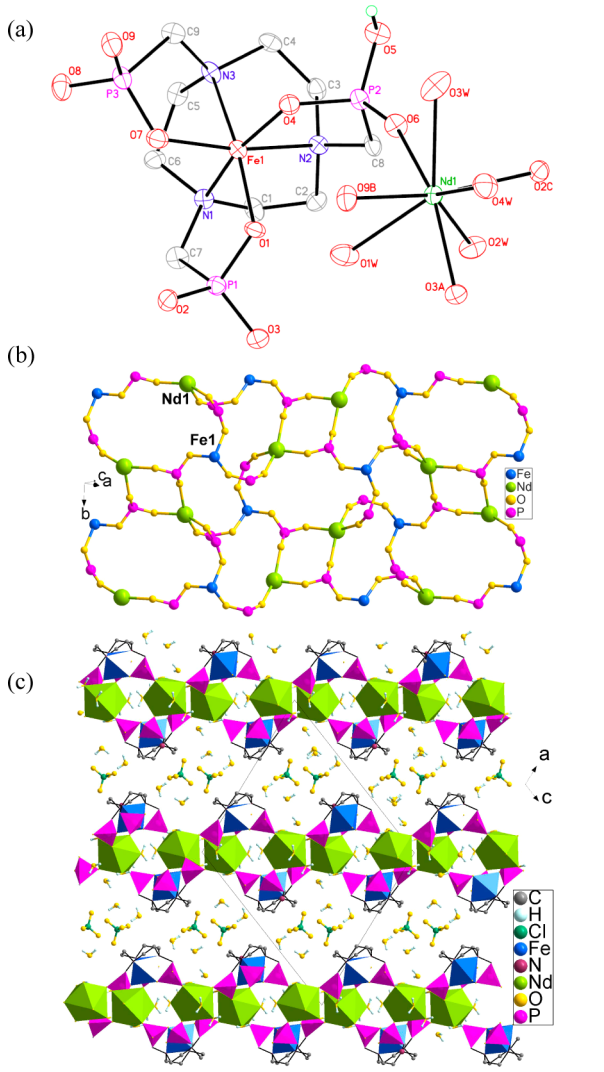

Figure 1. (a) Building unit of compound **FeNd** with atomic labeling scheme (50% probability). All hydrogen atoms except those attached to the phosphonate oxygen are omitted for clarity. (b) The 8- and 16-member rings in the layer of structure **FeNd**. (c) Structure **FeNd** packed along the *b*-axis. All H atoms except those attached to water molecules are omitted for clarity.

The layer structure of **FeLn** is also different from that of [ls-$Co^{III}La^{III}(notp)(H_2O)_4]\cdot nH_2O$ (**CoLa**)[7] in which the cobalt ion is also in the +3 state. In the latter case, however, all phosphonate oxygen atoms of $notp^{6-}$ are deprotonated. Thus, compound **CoLa** contains a neutral layer, separated by lattice water molecules, while, for compound **FeLn**, the layers are positively charged. The interlayer spaces are filled with both ClO_4^- and lattice water molecules.

Magnetic Properties. The temperature-dependent magnetic susceptibility data of compounds **FeLn** (Ln = Nd, Sm, Eu, Gd) were measured in the temperature range of 1.8–300 K under 100 Oe. The $\chi_M T$ versus T plots are shown in Figure 3.

For **FeNd**, **FeSm**, and **FeEu**, the room-temperature $\chi_M T$ values are 4.69, 4.51, and 5.60 cm^3 K mol^{-1}, respectively. The first one is smaller than the value expected (6.01 cm^3 K mol^{-1}) for one Fe^{III} ($g = 2.0$, $S = 5/2$) and one Nd^{III} ion ($^4I_{9/2}$, $g_J = 8/11$, $S = 3/2$), while the value for **FeSm** is close to 4.47 cm^3 K mol^{-1}, expected for one isolated Fe^{III} and Sm^{III} ion ($^6H_{5/2}$, $g_J = 2/7$, $S = 5/2$). The value for **FeEu**, however, is higher than that

dx.doi.org/10.1021/ic500356b | Inorg. Chem. 2014, 53, 6042–6047

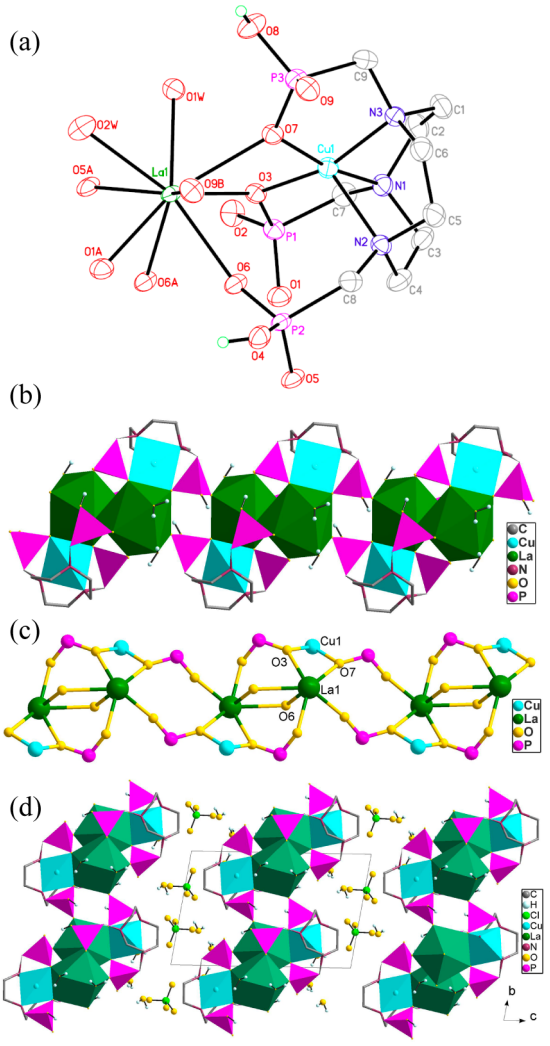

Figure 2. (a) Building unit of structure **CuLa** with atomic labeling scheme (50% probability). (b) A fragment of chain in structure **CuLa**. (c) The connection of the metal ions within the chain. (d) Packing diagram of structure **CuLa**. All hydrogen atoms attached to C are omitted for clarity.

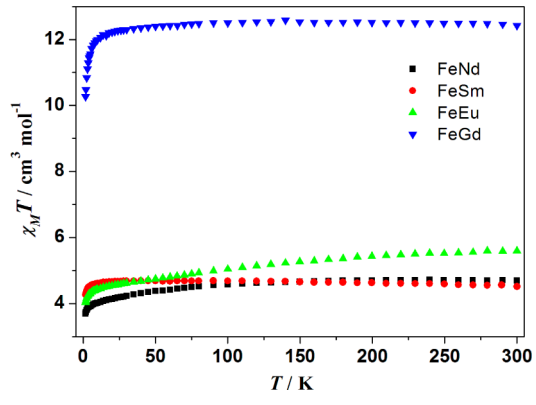

Figure 3. $\chi_M T$ vs T plots for compounds **FeLn** (Ln = Nd, Sm, Eu, Gd).

expected (4.38 cm^3 K mol^{-1}) for one Fe^{III} and one Eu^{III} ion ($^7F_0$, $g_J = 0$, $S = 3$) due to the thermally populated excited states of Eu^{III}. When the complexes are cooled, the $\chi_M T$ values of **FeNd** and **FeEu** decrease with decreasing temperature, while for **FeSm**, a small increase of $\chi_M T$ is observed on cooling to 45 K, below which the $\chi_M T$ value decreases sharply. Such magnetic behaviors could be attributed to the thermal depopulations of the Stark levels of the lanthanide ions, as well as a very weak antiferromagnetic/ferromagnetic exchange between the Fe^{III} and lanthanide ions over the phosphonate bridges.

For **FeGd**, the room-temperature $\chi_M T$ value of 12.42 cm^3 K mol^{-1} agrees well with the expected spin-only value for isolated Fe^{III} and Gd^{III} ($g = 2.0$, $S = 7/2$) ions (12.26 cm^3 K mol^{-1}). When this complex is cooled, the $\chi_M T$ value keeps almost constant until 20 K, below which it decreases sharply and reaches 10.27 cm^3 K mol^{-1} at 1.8 K. The behavior follows the Curie−Weiss law in the whole temperature range. The negative Weiss constant of −0.4 K suggests the presence of a very weak antiferromagnetic interaction propagated between the metal centers.

The magnetic susceptibility data of compound **CuLa** were recorded in the temperature range of 1.8−300 K under 2 kOe direct current field. The $\chi_M T$ and $\chi_M{}^{-1}$ versus T plots are given in Supporting Information, Figure S11. At room temperature, the magnetic moment per Cu is 1.83 μ_B, close to the value of 1.73 μ_B expected for an isolated spin of $S = 1/2$. The magnetic behavior follows the Curie−Weiss law in the whole temperature range with a small negative Weiss constant of −0.9 K, suggesting a very weak antiferromagentic coupling between the copper centers. The antiferromagnetic interaction is confirmed by the continuous decreasing of the $\chi_M T$ value upon cooling. The presence of a very weak antiferromagnetic exchange coupling in **CuLa** is reasonable, considering that the shortest Cu···Cu distances are 7.716(2) Å within the chain and 9.332(2) Å between the chains.

CONCLUSIONS

By using mononuclear compounds Fe(notpH$_3$) and Cu(notpH$_4$) as precursors, we succeeded in assembling five novel 3d−4f compounds including [FeLn(notpH)(H$_2$O)$_4$]ClO$_4$·5H$_2$O (Ln = Nd, Gd, Sm, Eu) with layer structures and [CuLa(notpH$_2$)(H$_2$O)$_2$]ClO$_4$·3H$_2$O with a chain structure. These are also the first examples of FeLn and CuLn phosphonates based on the notp^{6-} ligand. Further work is in progress to explore new 3d−4f materials containing phosphonate ligands with interesting magnetic and optical properties.

ASSOCIATED CONTENT

Supporting Information

Structural data, IR, and PXRD. This material is available free of charge via the Internet at http://pubs.acs.org.

AUTHOR INFORMATION

Corresponding Author

*E-mail: lmzheng@nju.edu.cn.

Notes

The authors declare no competing financial interest.

ACKNOWLEDGMENTS

This work is supported by the Natural Science Foundation of China (No. 11079021, 21101092) and the National Basic Research Program of China (2010CB923402, 2013CB922102).

REFERENCES

(1) (a) Ward, M. D. *Coord. Chem. Rev.* **2007**, *251*, 1663−1677. (b) Chen, F.-F.; Chen, Z.-Q.; Bian, Z.-Q.; Huang, C.-H. *Coord. Chem.*

Rev. **2010**, *254*, 991−1010. (c) Aboshyan-Sorgho, L.; Cantuel, M.; Petoud, S.; Hauser, A.; Piguet, C. *Coord. Chem. Rev.* **2012**, *256*, 1644−1663.
(2) (a) Winpenny, R. E. P. *Chem. Soc. Rev.* **1998**, 447−452. (b) Zhou, Y.; Hong, M.; Wu, X. *Chem. Commun.* **2006**, 135−143. (c) Evangelisti, M.; Brechin, E. K. *Dalton Trans.* **2010**, *39*, 4672.
(3) (a) Clearfield, A. *Prog. Inorg. Chem.* **1998**, *47*, 371−510. (b) Zheng, L.-M.; Song, H.-H.; Xin, X.-Q. *Comments Inorg. Chem.* **2000**, *22*, 129−149. (c) *Metal Phosphonate Chemistry: from Synthesis to Applications;* Clearfield, A., Demadis, K., Eds.; The Royal Society of Chemistry: London, U.K., 2012.
(4) (a) Baskar, V.; Gopal, K.; Helliwell, M.; Tuna, F.; Wernsdorfer, W.; Winpenny, R. E. P. *Dalton Trans.* **2010**, *39*, 4747. (b) Wang, M.; Yuan, D.-Q.; Ma, C.-B.; Yuan, M.-J.; Hu, M.-Q.; Li, N.; Chen, H.; Chen, C.-N.; Liu, Q.-T. *Dalton Trans.* **2010**, *39*, 7276. (c) Zheng, Y.-Z.; Evangelisti, M.; Winpenny, R. E. P. *Angew. Chem., Int. Ed.* **2011**, *50*, 3692. (d) Zheng, Y.-Z.; Evangelisti, M.; Winpenny, R. E. P. *Chem. Sci.* **2011**, *2*, 99. (e) Zheng, Y.-Z.; Pineda, E. M.; Helliwell, M.; Evangelisti, M.; Winpenny, R. E. P. *Chem.—Eur. J.* **2012**, *18*, 4161. (f) Zheng, Y.-Z.; Evangelisti, M.; Tuna, F.; Winpenny, R. E. P. *J. Am. Chem. Soc.* **2012**, *134*, 1057. (g) Pineda, E. M.; Tuna, F.; Pritchard, R. G.; Regan, A. C.; Winpenny, R. E. P.; McInnes, E. J. L. *Chem. Commun.* **2013**, *49*, 3522−3524.
(5) (a) Ma, Y.-S.; Li, H.; Wang, J.-J.; Bao, S.-S.; Cao, R.; Li, Y.-Z.; Ma, J.; Zheng, L.-M. *Chem.—Eur. J.* **2007**, *13*, 4759−4769. (b) Ma, Y.-S.; Song, Y.; Zheng, L.-M. *Inorg. Chim. Acta* **2008**, *361*, 1363−1371.
(6) Gu, Z.-G.; Sevov, S. C. *J. Mater. Chem.* **2009**, *19*, 8442−8447.
(7) Bao, S.-S.; Liao, Y.; Su, Y.-H.; Liang, X.; Hu, F.-C.; Sun, Z.; Zheng, L.-M.; Wei, S.; Alberto, R.; Li, Y.-Z.; Ma, J. *Angew. Chem., Int. Ed.* **2011**, *50*, 5504−5508.
(8) Bao, S.-S.; Chen, G.-S.; Wang, Y.; Li, Y.-Z.; Zheng, L.-M.; Luo, Q.-H. *Inorg. Chem.* **2006**, *45*, 1124−1129.
(9) Bao, S.-S.; Ma, L.-F.; Wang, Y.; Fang, L.; Zhu, C.-J.; Li, Y.-Z.; Zheng, L.-M. *Chem.—Eur. J.* **2007**, *13*, 2333−2343.
(10) Yu Antipin, M.; Baranov, A. P.; Kabachnik, M. I.; Ya Medved, T.; Polikarpov, Yu. M.; Struchkov, Yu. T.; Shcherbakov, B. K. *Dokl. Akad. Nauk SSSR* **1986**, *287*, 130.
(11) Kabachnik, M. I.; Yu Antipin, M.; K.Shcherbakov, B.; Baranov, A. P.; Struchkov, Yu. T.; YaMedved, T.; Polikarpov, Yu. M. *Koord. Khim.* **1988**, *14*, 536.
(12) (a) Wieghard, K.; Schmid, W.; Nuber, B.; Weiss, J. *Chem. Ber.* **1979**, *112*, 2220−2230. (b) Atkins, T. J.; Richman, J. E.; Oettle, W. F. *Org. Synth.* **1978**, *58*, 87.
(13) Kahn, O. *Molecular Magnetism;* VCH Publishers, Inc.: New York, 1993.
(14) *SAINT-Plus,* version 6.02; Bruker Analytical X-ray System: Madison, WI, 1999.
(15) Sheldrick, G. M. *SHELXTL-97;* Universität of Göttingen: Göttingen, Germany, 1997.
(16) (a) Song, J. L.; Lei, C.; Mao, J. G. *Inorg. Chem.* **2004**, *43*, 5630−5641. (b) Groves, J. A.; Wright, P. A.; Lightfoot, P. *Inorg. Chem.* **2005**, *44*, 1736−1739. (c) Liu, F. Y.; Roces, L.; Sa Ferreira, R. A.; Garcia-Granda, S.; Garcia, J. R.; Carlos, L. D.; Rocha, J. *J. Mater. Chem.* **2007**, *17*, 3696−3701. (d) Li, J.-T.; Zheng, L.-M. *Inorg. Chim. Acta* **2009**, *362*, 1739−1742.

dx.doi.org/10.1021/ic500356b | *Inorg. Chem.* 2014, 53, 6042−6047